LAWRENCE
LIVERMORE
NATIONAL
LABORATORY

LLNL-JRNL-416397

A Large-scale Relativistic Configuration-interaction Approach: Application to the 4s2 - 4s4p Transition Energies and E1 Rates for Zn-like Ions

M. H. Chen, K. T. Cheng

September 1, 2009

Journal of Physics B

Disclaimer

A large-scale relativistic configuration-interaction approach: application to the $4s^2 - 4s4p$ transition energies and E1 rates for Zn-like ions

M H Chen and K T Cheng

Lawrence Livermore National Laboratory, Livermore, CA 94550, USA

E-mail: chen7@llnl.gov

Abstract. Relativistic configuration-interaction calculations of the $4s4p$ excitation energies and $4s^2 - 4s4p$ E1 transitions for Zn-like ions from $Z = 30$ to 92 are shown. B-spline basis functions are used for these large-scale calculations. QED corrections to the excitation energies are also calculated. Results are in good agreement with other theories and with experiment, and demonstrate the utility of this method for high-precision atomic structure calculations not just for few-electron systems but also for large atomic systems such as Zn-like ions along the entire isoelectronic sequence.

PACS numbers: 31.15.am, 31.30.jf, 32.70.Cs

1. Introduction

For high-precision atomic structure calculations, two aspects of many-electron systems have always been the foci of intense theoretical investigations. The first is the relativistic electron-electron correlation energy and the other is the quantum electrodynamic (QED) correction. Rigorous and consistent treatment of these two problems should come from S-matrix calculations and this approach has been used to study the $n = 2$ energy levels of Li-like ions [1, 2]. However, it is very difficult, if not impossible, to extend this perturbative method to more electron systems, especially for non-alkalilike ions. The alternative is to treat the correlation and QED problems separately. This is the approach taken by most of the existing atomic structure theories which deal primarily with relativistic correlation energies from electron-electron interactions. QED corrections, which are dominated by radiative corrections from electron self-energies and vacuum polarizations, can be accurately calculated for low-Z ions using weak-field, $Z\alpha$-expansion methods [3, 4]. For high-Z many-electron ions, however, the strong nuclear fields must be treated to all orders in the $Z\alpha$ expansion and nonperturbative methods are needed. To date, this problem has largely been overcome and *ab initio* calculations of the Lamb shifts can now be carried out routinely for heavy atoms and ions. Nevertheless, rigorous treatments of screening and relaxation corrections to QED energies such as those given in [1, 2] for Li-like ions are rare and these effects are usually accounted for approximately by using model potentials in calculating the lowest-order, one-loop radiative corrections [5, 6] or by truncating the screened QED calculations [7]. Furthermore, higher-order QED corections such as two-loop Lamb shifts remain relatively unstudied [1, 8, 9]. Accurate relativistic atomic structure calculations are thus crucial to the testing of strong-field QED effects where screening and higher-order corrections can be important.

Multiconfiguration Dirac-Fock (MCDF) calculations such as those based on the GRASP code [10] have been the work horse for relativistic atomic structure calculations for many-electron atomic systems, though advances have been made to go beyond the MCDF method to account more accurately for relativistic correlation corrections. One such approaches is the relativistic many-body perturbation theory (RMBPT) developed by Johnson, Blundell and Sapirstein [11, 12, 13]. Another approach is the relativistic configuration-interaction (RCI) method with finite B-spline basis functions originally developed by Chen, Cheng and Johnson for He-like ions [14] and later generalized to three or more electron systems [15, 16]. Reviews of RMBPT can be found in [17] and RCI in [17, 18]. Both methods treat relativistic and many-electron correlation effects on an equal footing and work equally well for low- and high-Z ions, though RCI, with its variational approach, may be more readily applicable to systems with multiple open-shell electrons.

In this paper, we shall demonstrate the utility of the RCI method for high-precision atomic structure calculations by applying it to study the $4s4p\ ^3P_{0,1,2}$ and $^1P_1$ excitation energies and E1 decay rates of the $4s4p\ ^{1,3}P_1$ states to the $4s^2\ ^1S_0$ ground state for ions in the Zn isoelectronic sequence. In the next section, we shall first give a brief

descriptions of this method. Computational details pertinent to the Zn-like ions will then be presented in section 3.2, followed by results and discussions of the present calculations.

2. Theory

2.1. The no-pair Hamiltonian

Relativistic atomic structure calculations pose subtle conceptual difficulties as well as formidable technical challenges. They usually start from the N-electron Dirac Hamiltonian that is given in the Coulomb gauge by

$$H_{\rm Dirac} = \sum_{i=1}^{N} h_i + (H_{\rm C} + H_{\rm B}), \tag{1}$$

where

$$h_i = c\,\boldsymbol{\alpha}_i \cdot \boldsymbol{p}_i + (\beta_i - 1)mc^2 + V_{\rm nuc}(r_i) \tag{2}$$

is the one-electron Dirac Hamiltonian with the rest mass of the electron subtracted out,

$$H_{\rm C} = \sum_{i>j} \frac{e^2}{r_{ij}} \tag{3}$$

is the Coulomb interaction between the electrons, and

$$H_{\rm B} = -\sum_{i>j} \frac{e^2}{r_{ij}} \left[\boldsymbol{\alpha}_i \cdot \boldsymbol{\alpha}_j \cos k_0 r_{ij} - (\boldsymbol{\alpha}_i \cdot \boldsymbol{\nabla}_i)(\boldsymbol{\alpha}_j \cdot \boldsymbol{\nabla}_j) \frac{\cos k_0 r_{ij} - 1}{k_0^2} \right] \tag{4}$$

is the frequency-dependent Breit interaction with $k_0 = \omega/c$. The nuclear potential is given by $V_{\rm nuc}(r) = -Ze^2/r$ for point-Coulomb potentials, but it can be modified to include nuclear charge distributions to account for finite nuclear size corrections.

While the many-electron Dirac Hamiltonian is widely used in relativistic atomic structure calculations including the MCDF method, it is nevertheless known to be problematic. Specifically in relativistic calculations, the existence of negative-energy states, which enter into sums over intermediate states in perturbation theory, results in the "continuum dissolution" problem, also known as the Brown-Ravenhall disease [19], in many-electron systems. Discussions of this problem can be found, for example, in [18] and will not be repeated here. To avoid this problem, we employ the no-pair Hamiltonian

$$H_{\rm no-pair} = \sum_{i=1}^{N} h_i + \Lambda_{++}(H_{\rm C} + H_{\rm B})\Lambda_{++} \tag{5}$$

which excludes negative-energy states entirely by the use of the positive-energy projector Λ_{++} [20, 21, 22, 23]. This is the starting point of our RCI calculations, as it should be for any high-precision relativistic atomic structure calculations. Contributions from the negative-energy states can be obtained from S-matrix calculations and should be considered as part of the QED corrections [18]. These are very small corrections and have been shown to be comparable in size to higher-order, two-loop Lamb shifts in high-Z Li-like ions [18]. In most cases, they can simply be ignored.

2.2. The CI equation

The eigenfunction $\Psi(J^\pi M)$ of an atomic state with angular momentum (J, M) and parity π is expressed as a linear combination of the many-electron configuration-state functions $\phi(\Gamma_i JM)$ such that

$$\Psi(J^\pi M) = \sum_i c_i \phi(\Gamma_i JM), \tag{6}$$

where Γ_i are sets of quantum numbers representing different electronic configurations with the same parity π, and c_i are configuration mixing coefficients. Variation of the energy functional $\langle\Psi|H|\Psi\rangle$ with respect to c_i, subjected to the wavefunction normalization condition, leads to the CI equation

$$\sum_j (H_{ij} - \lambda\delta_{ij})c_j = 0. \tag{7}$$

Expressions for the matrix elements H_{ij} in terms of the configuration-state functions are given in [15].

2.3. B-spline basis functions

For our RCI calculations, we use the B-spline finite basis set method developed by Johnson *et al* [24]. B-spline orbitals are Dirac orbitals of an electron moving in a model potential confined to a finite cavity. They are expanded in terms of B-spline, or basis-spline, functions which are piecewise polynomials in an interval divided into segments, and expansion coefficients are obtained by solving a generalized eigenvalue problem set up by the one-electron Dirac equation subjected to the boundary condition imposed by the MIT bag model [25] at the cavity boundary to ensure that the electrons are confined without evoking the difficulty associated with the Klein paradox [26].

B-spline orbitals form finite, complete basis sets as confirmed by sum rule calculations [24]. They also cleanly separated into positive- and negative-energy states so that the no-pair requirement can easily be implemented by using only positive-energy B-spline orbitals which readily provide an accurate, discrete representation of the bound and continuum states for high-precision correlation calculations. There are also no low-lying spurious states in the one-electron spectra and no known variational instability problems suffered by earlier relativistic basis set calculations [27, 28]. With configuration-state functions constructed from positive-energy B-spline orbitals, correlation contributions from single, double, triple, ... excitations can be systematically included in the form of valence-valence, core-valence, core-core, ... excitations for very well converged RCI results. The down side of this approach is that B-spline basis functions are not highly optimized and can lead to big basis sets and very large-scale RCI expansions. But with advances in high-performance computers, this is no longer an insurmountable problem. Recent RCI calculations using B-spline basis functions have reached close to half a million configurations, and the iterative Davidson method [29] as implemented by Stathopoulos and Froese Fischer [30] is used to solve these large RCI matrices for the first few eigenvalues.

2.4. Radiative transitions

In this work, radiative transition rates are calculated from the frequency-dependent electromagnetic multipole transition operator [31, 32]. Angular recoupling coefficients used in the present E1 transition calculations are computed with the MCT package from the Oxford MCDF code [33] that is consistent with the MCP angular recoupling package, also from the same MCDF code, used in our RCI energy calculations. Since the most time-consuming part of these large-scale transition rate calculations is in the evaluation of millions and millions of angular recoupling coefficients that are largely independent of the principal quantum numbers n of the basis functions, we use an angular channel scheme, similar to the one used to speed up our RCI energy calculations, such that only angular coefficients from distinct angular channels are evaluated [15, 16]. It should be noted that neglecting negative-energy states in no-pair calculations has been shown to lead to gauge-dependent transition rates, especially for spin-forbidden, intercombination transitions at low Z, and that length-gauge results have been found to be quite unaffected by this problem [34]. We thus use length gauge for our transition calculations here.

2.5. QED calculations

QED corrections are important for high-precison excitation and transition energy calculations, especially for high-Z ions. They are dominated by one-loop radiative corrections from electron self-energy and vacuum polarization. In this work, electron self-energies are calculated nonperturbatively to all orders of $Z\alpha$ in an external potential with partial wave expansions in the configuration space using numerical bound-state Green's functions. Subtraction terms arising from mass renormalization and involving free-electron propagators are evaluated in momentum space with Fourier-transformed wavefunctions. Details of these self-energy calculations can be found in [5]. As for the vacuum polarization, leading contributions are obtained from expectation values of the Uehling potential, while higher-order Wichmann-Kroll corrections, like the self-energies, are calculated nonperturbatively in an external potential with partial wave expansions in the configuration space using numerical bound-state Green's functions [6]. Total QED corrections are then given by sums of one-electron QED contributions, weighted by the generalized occupation numbers of the valence electrons as given by atomic structure calculations.

3. Application to the zinc isoelectronic sequence

For the excitation energies of the $4s4p\ ^3P_{0,1,2}$ and $^1P_1$ states from the $4s^2\ ^1S_0$ ground state of Zn-like ions, there exist many experimental and theoretical studies. For low- to mid-Z ions ($Z \simeq 30 - 54$,) empirical data can be found in the NIST database [35] for $Z = 30 - 37$, 42 and 54, from Litzen and Reader [36] for $Z = 37 - 42$, from Joshi and van Kleef [37] for $Z = 34, 35$, from Trigueiros *et al* [38] for $Z = 36$ and from Churilov *et*

al [39] for $Z = 37 - 50$. Among the more accurate calculations in this Z range are the MCDF results of Liu *et al* [40] for $Z = 30 - 47$ which agree with experiment to within 0.1 – 0.2 eV.

For mid- to high-Z ions ($Z \simeq 50-92$), early experimental results were obtained from the spectra of laser-produced plasmas [41, 42, 43, 44] and tokamak discharges [45, 46, 47]. Early calculations were based on the MCDF method [43, 48, 49, 50], the Hebrew University-Lawrence Livermore Atomic code (HULLAC) [44], the semi-relativistic Cowan code [51] and the multiconfiguration relativistic random-phase approximation (MCRRPA) [52]. Non of these calculations were particularly accurate, and typical agreement between theory and experiment was at a few tenths of an eV level.

More recently, Utter *et al* [53] and Träbert *et al* [54] have carried out high-precision Electron Beam Ion Trap (EBIT) measurements of the EUV resonance line $4s^2\ {}^1S_0 - 4s4p\ {}^1P_1$ of Zn-like ions between $Z = 70 - 92$. Accuracies of these experiments are about 0.02 eV out of 200 – 500 eV, putting them at or below the 0.01% level, enough for stringent tests of relativistic correlation energies and QED corrections in strong nuclear fields. On the theoretical front, Vilkas and Ishikawa [55] have carried out accurate calculations of the $4s4p$ energies in the same Z range using the relativistic multi-reference Moller-Plesset (MR-MP) perturbation theory, though their results still differ from the EBIT measurements by as much as 0.15 eV. Recently, Blundell *et al* [56] carried out a comprehensive study of the even- and odd-parity $4l4l'$ energies along the Zn isoelectronic sequence using the second-order RMBPT method. However, the use of frequency-independent, unretarded Breit interaction and, to a lesser extent, incomplete treatments of correlation corrections to QED energies severely affect the accuracy of their results at high Z. Later, Blundell [57] recalculated the ${}^1P_1$ excitation energies for high-Z Zn-like ions by including frequency-dependent, retarded Breit corrections and improving the QED calculations, and his revised results are in much better agreement with the high-precision EBIT measurements [54].

Regarding the $4s^2 - 4s4p$ E1 transition rates, experiments were performed using mostly beam-foil spectroscopy with about 10% accuracy. Existing calculations were carried out using multiconfiguration Hartree-Fock (MCHF) [58], RRPA [59], MCRRPA [52] and MCDF [40] methods. Since theoretical energies from these works are generally not very accurate, their transition rates typically need empirical energy adjustments [60] to reach fair agreements with experiment. Details of these adjustments will be given in the following.

In this work, we apply the RCI theory described in section 2 to the calculations of $4s4p$ excitation energies and E1 decay rates for Zn-like ions along the entire isoelectronic sequence. QED corrections to the excitation and transition energies are also calculated. Details of our numerical calculations will be given in the next section. Results of this work will be presented and compared with other theories and with experiment in section 3.2.

3.1. Computational details

Our B-spline basis functions are calculated in Dirac-Kohn-Sham (DKS) potentials of Zn-like ground state with a box size of 40 a.u. for zinc ($Z = 30$) and 3 a.u. for uranium ($Z = 92$). In between, an inverse scaling law with Z is applied. In our RCI calculations, nuclear charge distributions are included in the nuclear potential $V_{\rm nuc}(r)$ for generating one-electron B-spline basis functions to account for the finite nuclear size effect. Parameters for the Fermi charge distributions are obtained from Johnson and Soff [61], except for thorium and uranium that are obtained from the measurements by Zumbro *et al* [62, 63]. Typically, 35 positive-energy B-spline orbitals for each of the angular symmetries $s, p_{1/2}, p_{3/2}, \ldots$ are generated and the first 20 orbitals are used in our RCI calculations. Contributions from higher-n orbitals are found to be quite negligible.

Zn-like configurations consist of core and valence electrons. The core is defined as a Ni-like ground state configuration containing the closed $1s, 2s, 2p, 3s, 3p, 3d$ subshells, and valence electrons come from the $4s, 4p, 4d$ subshells. Our calculations start from the reference configurations $4s^2 + 4p^2$ for the ground state and $4s4p + 4p4d$ for the excited states. For simplicity, the Ni-like core is not listed here. In our basic CI expansions, we include single and double excitations from these reference configurations. B-spline orbitals with $n \leq 20$ and $l \leq 5$ are used to form configuration-state functions that correspond to valence-valence (VV) and core-valence (CV) excitations of the $3p, 3d$ core and $4s, 4p, 4d$ valence electrons. CV contributions from inner core electrons are small and are calculated separately as corrections with smaller basis sets of $n \leq 20$ and $l \leq 3$ for the $2s, 2p, 3s$ core and $4s, 4p$ valence electrons. Remaining CV excitations from the $1s$ subshell and core-core (CC) excitations are found to contribute less than 0.01 eV to the excitation energies and are neglected here. The present CI expansions reach almost 300 000 configurations and Davidson's method [29, 30] is used to solve for the lowest few eigenstates of the even parity $J = 0$ and odd parity $J = 0, 1, 2$ CI matrices. E1 transition rates are then calculated with RCI eigenvectors, though RCI transition energies do include QED corrections.

As the frequency-dependent, retarded Breit interaction is much more time consuming to evaluate than the frequency-independent, unretarded Breit interaction, we include the former in diagonal RCI matrix elements only while the latter is used in off-diagonal matrix elements. This gives the dominant "diagonal" contributions to frequency-dependent Breit energies. "Off-diagonal" contributions are then determined in separate calculations using smaller CI expansions from more restricted VV excitations. Results show that off-diagonal terms are much smaller than diagonal terms and can definitely be treated as perturbations.

RCI calculations are computer intensive and it is not practical to carry them out for every Zn-like ion along the isoelectronic sequence. Instead, they are carry out for 28 ions in the range $30 \leq Z \leq 92$. MCDF calculations of excitation energies and E1 transition rates are then carried out for all Zn-like ions in this Z range using the extended average level (EAL) scheme [33] including all $4l4l'$ configurations from the

$4s$, $4p$ and $4d$ electrons. Differences between RCI and MCDF excitation energies and transition line strengths are then interpolated to obtain RCI correlation corrections for all Z. MCDF results thus corrected are essentially the same as those from direct RCI calculations and are referred to as RCI results here.

In our QED calculations, Dirac-Kohm-Sham (DKS) potentials are used to account for screening effects in self-energy (SE), Uehling potential (UP) and Wichmann-Kroll (WK) corrections. In a frozen-core approximation, the same $4s^2$ DKS potential is used for the ground and excited states and there is no contributions from the closed Ni-like core as its QED energies cancel exactly between the initial and final states. To account for relaxation effects from the core and valence electrons, DKS potentials specific to the ground and excited states are used. Their configurations consist of $4s$, $4p$ and $4d$ valence electrons with fractional occupation numbers as determined by the above mentioned MCDF calculations. As we shall show in the following, relaxation effects, though small, are important in bringing theory into better agreement with experiment for high-Z Zn-like ions. Finally, higher-order QED corrections are based mainly on estimates of two-loop Lamb shifts. They are very small and should be considered as order-of-magnitude estimates only. We note that QED corrections to transition rates are limited to energy corrections only. Radiative corrections to transition matrix elements are not considered here.

3.2. Results and discussions

As an illustration of various contributions to the total energy, we show in table 1 breakdowns of RCI and QED excitation energies for four Zn-like ions. They are dominated by Coulomb energies, though Breit and QED corrections increase rapidly with Z and become more important at high Z. It is interesting to note that for U^{62+}, frequency-dependent corrections contribute only about 3% to the total Breit energies for the $^3P_0$ and $^3P_1$ states, which is quite normal, but more than 50% for the $^3P_2$ and $^1P_1$ states, which is surprisingly large. This is apparently due to the fact that in the high-Z jj-coupling limit, the $^3P_0$ and $^3P_1$ states become a $4s4p_{1/2}$ doublet while the $^3P_2$ and $^1P_1$ states become a $4s4p_{3/2}$ doublet. Contributions to the excitation energies thus come mainly from energy differences between the $4p_{1/2}$ electron from the two lower excited states or the $4p_{3/2}$ electron from the two upper excited states with the $4s$ electron from the ground state, hence the similarities in contributions between the $^3P_0$ and $^3P_1$ states and between the $^3P_2$ and $^1P_1$ states. Furthermore, degrees of cancelations for the frequency-independent (B_0) and frequency-dependent (B_ω) Breit energies between the $4p_{1/2}$ and $4s$ electrons are different from those between the $4p_{3/2}$ and $4s$ electrons, resulting in the changing importance of B_ω between these two groups of doublets. We note that QED excitation energies are also determined mainly by cancelations between the $4p$ and $4s$ electrons. But as contributions from $4p_{1/2}$ and $4p_{3/2}$ are both small compared to those from $4s$, QED corrections are dominated by the latter and are thus similar in size among all four $4s4p$ states along the entire isoelectronic sequence.

In tables 2 – 5, we list RCI, QED and total excitation energies for the $^3P_0$, $^3P_1$, $^3P_2$, and $^1P_1$ states, respectively, for all Zn-like ions in the range $30 \leq Z \leq 92$. Uncertainties of the RCI energies are estimated to be about 0.03 eV for all ions. They come mostly from the uncalculated CV (from the $1s$ subshell), CC, triple and quadruple excitations. Contributions from the also uncalculated nuclear recoil, nuclear polarization and negative-energy states should be quite negligible. Uncertainties in QED energies range from 0.006 eV for low-Z ions to 0.02 eV for mid-Z ions to 0.04 eV for high-Z ions. They come from the approximated treatment of screening and relaxation effects and from estimates of higher-order QED corrections. The combined uncertainties of the excitation energies are $\sim$0.03 eV for low-Z ($30 \leq Z \leq 40$), $\sim$0.04 eV for mid-Z ($40 < Z < 70$) and $\sim$0.05 eV for high-Z ($Z \geq 70$) ions.

In figures 1 – 4, we compare excitation energies for the $^3P_0$, $^3P_1$, $^3P_2$, and $^1P_1$ states, respectively, with other theories [40, 52, 55, 56, 57] and with experiments [35, 36, 37, 38, 39, 44]. For low- to mid-Z ions, our excitation energies agree with those from the NIST database [35], Litzen and Reader [36] and Churilov *et al* [39] to within 0.03 eV for all states. Exceptions are the discrepancies with NIST at Br^{5+} for the $^3P_{0,1,2}$ and at Xe^{24+} for the $^3P_{0,2}$ states which range from 0.05 to 0.1 eV, though our results for Br^{5+} do agree with the data in Joshi and van Kleef [37] to within 0.02 eV. In general, our results agree better with experiment than the RMBPT results of Blundell *et al* [56] and the MCDF results of Liu *et al* [40] in this part of the isoelectronic sequence, especially for the $^1P_1$ state. It is interesting to note that while discrepancies of RCI and RMBPT with experiment remain fairly constant in this Z range, discrepancies between MCDF and empirical data actually grow as functions of Z. The reason for this trend is unknown, as no breakdowns of contributions are given in that work.

At high Z, the MR-MP results of Vilkas and Ishikawa [55] seem to scatter around our results by as much as 0.2 eV. The RMBPT results of Blundell *et al* [56], on the other hand, systematically deviated more and more from our results as Z increases and discrepancies reach over 0.5 eV for the $^3P_2$ and $^1P_1$ states. The revised RMBPT $^1P_1$ energies of Blundell [57] are in much better agreement with our results, with discrepancies reduced by an order-of-magnitude to no more than 0.05 eV. More importantly, both our RCI and Blundell's revised RMBPT results on the total $^1P_1$ energies are in excellent agreement with the high-precision EBIT measurements [54].

The dramatic improvement in RMBPT results at high Z comes from two changes made in [57]: better QED calculations and the inclusion of frequency-dependent, retarded Breit corrections. In table 6, we compare *ab initio* QED energies calculated here with those from Blundell *et al* [56] and Blundell [57]. Our QED energies lie between the other two theoretical predictions and are slightly closer to Blundell's revised results [57], with differences ranging from 0.02 to 0.05 eV. In view of the difficulty of these QED calculations, the agreement among theories is quite reasonable. Nevertheless, Blundell's new QED results actually increase the RMBPT $^1P_1$ total energy and worsen the discrepancy with RCI and EBIT measurements by 0.14 eV for U^{62+}.

As for the frequency-dependent, retarded Breit corrections for the $^1P_1$ state,

we compare in table 7 our RCI results with those from Blundell's revised RMBPT calculations [57]. Diagonal frequency-dependent Breit corrections from the present work are in excellent agreement with Blundell's retardation corrections. Off-diagonal corrections are small, and are apparently not included in Blundell's calculations. In general, frequency-dependent Breit corrections are small parts of the total Breit corrections and can often be neglected. As shown in table 1, this is certainly true with the $^3P_0$ and $^3P_1$ states here, but not so with the $^3P_2$ and $^1P_1$ states where these corrections are surprisingly large as pointed out earlier. At –0.1 to –0.5 eV for $Z = 70$ to 92, the inclusion of these corrections also bring RMBPT $^1P_1$ correlation energies to agree with RCI to within 0.03 eV. Along with the revised QED corrections, the RMBPT $^1P_1$ total energies are in very good agreement with RCI and EBIT measurements as shown in figure 4. Blundell's revised RMBPT results underscore the importance of accurate evaluations of QED and Breit corrections in high-precision calculations, especially for high-Z ions.

We note that early RMBPT $^1P_1$ energies of Blundell *et al* [56] actually agree very well with the laser-plasma measurements of Brown *et al* [44] for $Z > 69$ as shown in figure 4, but that was clearly accidental. Indeed, laser-plasma results appear to drift to higher and higher energies as Z increases and the same trend is found in the $4s - 4p$ transition energies in Cu-like ions where laser-plasma results [64] are systematically higher than high-precision EBIT measurements [65] and RCI calculations [66] by 0.1 to 0.5 eV for $Z = 74 - 92$.

In table 8, transition rates from our RCI calculations are listed. As mentioned earlier, they are calculated in the length gauge with RCI total transition energies that include QED corrections. In tables 9 and 10, radiative lifetimes of the $^1P_1$ and $^3P_1$ states, respectively, are compared with other theories and with experiment. Since theoretical energies may not be very accurate, theoretical transition rates, which scale like ω^3, are often adjusted by replacing theoretical with empirical transition energies. For low- to mid-Z ions, the $4s^2\ ^1S_0 - 4s4p\ ^3P_1$ spin-forbidden transition is allowed through singlet-triplet mixings and its transition matrix element is proportional to the small $^1P_1$ mixing coefficient which in turn scales approximately like the inverse of the $^{1,3}P_1$ level splitting. As a result, radiative lifetimes are often scaled by the transition energy $\Delta E = E(^{3,1}P_1) - E(^1S_0)$ with the formula

$$\tau_{\rm adjusted} = \tau_{\rm original}\,(\Delta E_{\rm theory}/\Delta E_{\rm expt})^3\,, \tag{8}$$

while those for the $^3P_1$ states may be further scaled by the singlet-triplet interval energy $\delta E = E(^1P_1) - E(^3P_1)$ with the formula [60]

$$\tau_{\rm adjusted} = \tau_{\rm original}\,(\Delta E_{\rm theory}/\Delta E_{\rm expt})^3\,(\delta E_{\rm expt}/\delta E_{\rm theory})^2\,. \tag{9}$$

In tables 9 and 10, theoretical results from CIV3 [60, 67] and MCDF [40] have already been adjusted with empirical transition energies in those works, and the CIV3 $^3P_1$ lifetimes have further been adjusted with the singlet-triplet splittings. MCRRPA [52] and MCHF [58] results, on the other hand, are obtained from the gf values listed in those works and are converted to radiative lifetimes with empirical transition energies

only. Since our RCI energies and singlet-triplet splittings agree better than 0.5% with empirical data even for neutral zinc, we do not make empirical energy adjustment to our RCI results which are entirely from *ab initio* calculations.

For the lifetimes of the $^1P_1$ state, the agreement among theories and experiment is within 10%. For the lifetimes of the $^3P_1$ states, the agreement is also within 10% except for neutral zinc (as large as 50%) and singly-ionized Ga^+ ($\sim$20%). This shows the sensitivity of the intercombination transition on electron correlations, as these spin-forbidden $^3P_1$ transition rates depends critically on the mixing with the $^1P_1$ state for low-Z ions. Indeed, if no energy adjustment is made, the $^3P_1$ lifetimes from MCRRPA [52] would be larger than the RCI lifetimes by a factor of 2.2 for zinc and 16% for Kr^{6+} ion, while the CIV3 lifetime for Ga^+ would be larger by 60% [60]. Our present RCI energies are accurate enough that energy adjustments are quite unnecessary.

4. Conclusion

We have shown that the present RCI theory yields quite accurate relativistic correlation energies even for large atomic systems such as 30-electron Zn-like ions. Combining our *ab initio* RCI and QED energies, theoretical excitation energies agree with experiments to better than 0.05 eV for all $4s4p$ excited states along the entire isoelectronic sequence. By comparing with high-precision EBIT measurements of the spectra of high-Z ions, RCI results can provide important tests of strong field QED. At present, we have applied the RCI theory mostly to systems with one or two valence electrons. For many-open-shell complex systems, a more efficient many-electron theory and/or more compact and efficient basis functions will be needed for high-precision atomic structure calculations. We have calculated the lowest-order QED energies including screening and relaxation effects for Zn-like ions. To improve the accuracy, higher-order QED corrections are desirable.

Acknowledgments

Work performed under the auspices of the U.S. Department of Energy by Lawrence Livermore National Laboratory under Contract DE-AC52-07NA27344.

References

[1] Sapirstein J and Cheng K T 2001 *Phys. Rev.* A **64** 022502.
[2] Yerokhin V A, Artemyev A N, Shabaev V M, Sysak M M, Zherebtsov O M and Soff G 2001 *Phys. Rev.* A **64** 032109.
[3] Yan Z C and Drake G W F 2003 *Phys. Rev. Lett.* **91** 113004.
[4] Puchalski M and Pachucki K 2006 *Phys. Rev.* A **73** 022503.
[5] Sapirstein J and Cheng K T 2006 *Phys. Rev.* A **73** 012503.
[6] Sapirstein J and Cheng K T 2003 *Phys. Rev.* A **68** 042111.
[7] Blundell 1992 *Phys. Rev.* A **46** 3762.
[8] Beiersdorfer P, Chen H, Thorn D B and Träbert E 2005 *Phys. Rev. Lett.* **95** 233003.

[9] Yerokhin V A, Indelicato P and Shabaev V M 2006 *Phys. Rev. Lett.* **97** 253004.
[10] Dyall K G, Grant I P, Johnson C T, Parpia F A and Plummer E P 1989 *Comp. Phys. Commun.* **55** 425.
[11] Johnson W R, Blundell S A and Sapirstein J 1988 *Phys. Rev.* A **37** 2764.
[12] Johnson W R, Blundell S A and Sapirstein J 1988 *Phys. Rev.* A **38** 2699.
[13] Johnson W R, Blundell S A and Sapirstein J 1990 *Phys. Rev.* A **42** 1087.
[14] Chen M H, Cheng K T and Johnson W R 1993 *Phys. Rev.* A **47** 3692.
[15] Chen M H, Cheng K T, Johnson W R and Sapirstein J 1995 *Phys. Rev.* A **52** 266.
[16] Chen M H and Cheng K T 1997 *Phys. Rev.* A **55** 166.
[17] Johnson W R, Cheng K T and Chen M H 2004 Accurate relativistic calculations including QED contributions for few-electron systems *Relativistic Electronic Structure Theory Part 2 Applications* vol 14 *Theoretical and computational chemistry* ed P Schwerdtfeger (Elsevier).
[18] Cheng K T, Chen M H, Johnson W R and Sapirstein J 2008 *Can. J. Phys.* **86** 33.
[19] Brown G E and Ravenhall D G 1951 *Proc. R. Soc. London* Series A **208** 552.
[20] Sucher J 1980 *Phys. Rev.* A **22** 348.
[21] Mittleman M H 1971 *Phys. Rev.* A **4** 893.
[22] Mittleman M H 1972 *Phys. Rev.* A **5** 2395.
[23] Mittleman M H 1981 *Phys. Rev.* A **24** 1167.
[24] Johnson W R, Blundell S A and Sapirstein J 1988 *Phys. Rev.* A **37** 307.
[25] Chodos A, Jaffe R L, Johnson K, Thorn C B and Weisskopf V W 1974 *Phys. Rev.* D **9** 3471.
[26] Sakurai J J 1967 *Advanced Quantum Mechanics* (Reading, Massachusetts: Addison-Wesley).
[27] Mark F and Schwarz W H E 1982 *Phys. Rev. Lett.* **48** 673.
[28] Stanton R E and Havriliak S 1984 *J. Chem. Phys.* **81** 1910.
[29] Davidson E R 1975 *J. Comp. Phys.* **17** 87.
[30] Stathopoulos A and Fischer C F 1994 *Comput. Phys. Commun.* **79** 1.
[31] Johnson W R, Plante D R and Sapirstein J 1995 *Advances in Atomic, Molecular and Optical Physics* ed B Bederson and H Walther (San Diego: Academic) p 251.
[32] Grant I P 1974 *J. Phys. B: At. Mol. Opt. Phys.* **7** 1458.
[33] Grant I P, McKenzie B J, Norrington P H, Mayers D F, and Pyper N C 1980 *Comput. Phys. Commun.* **21** 207.
[34] Chen M H, Cheng K T, and Johnson W R 2001 *Phys. Rev.* A **64** 042507.
[35] NIST Atomic Spectra Database, http://physics.nist.gov/PhysRefData/ASD.
[36] Litzen U and Reader J 1987 *Phys. Rev.* A **36** 5159.
[37] Joshi Y N and van Kleef T A M 1986 *Phys. Scr.* **34** 135.
[38] Trigueiros A, Pettersson S G and Reyna Almandos J G 1986 *Phys. Scr.* **34** 164.
[39] Churilov S S, Ryabtsev A N and Wyart J F 1988 *Phys. Scr.* **38** 326.
[40] Liu Y, Hutton R, Zou Y, Anderson M and Brage T 2006 *J. Phys. B: At. Mol. Opt. Phys.* **39** 3147.
[41] Reader J and Luther G 1980 *Phys. Rev. Lett.* **45** 609.
[42] Acquista N and Reader J 1984 *J. Opt. Soc. Am.* B **1** 649.
[43] Seely J F, Ekberg J O, Brown C M, Feldman U, Behring W E, Reader J and Richardson M C 1986 *Phys. Rev. Lett.* **57** 2924.
[44] Brown C M, Seely J F, Kania D R, Hammel B A, Back C A, Lee R W, Bar-Shalon A and Behring W E 1994 *At. Data Nucl. Data Tables* **58** 203.
[45] Hinnov E, Beiersdorfer P, Bell R, Stevens J, Suckewer S, von Goeler S, Wouters A, Dietrich D, Gerassimenko M and Silver E 1987 *Phys. Rev.* A **35** 4876.
[46] Sugar J, Kaufman V, Balk D H, and Kim Y K 1991 *J. Opt. Soc. Am.* **B8** 1795.
[47] Sugar J, Kaufman V, and Rowan L 1993 *J. Opt. Soc. Am.* **B10** 799.
[48] Cheng K T and Wagner R A 1987 *Phys. Rev.* A **36** 5435.
[49] Biemont E 1989 *At. Data. Nucl. Data Tables* **43** 163.
[50] Indelicato P and Desclaux 1990 *Phys. Rev.* A **42** 5139.
[51] Biemont E, Quinet P, and Fawcett B C 1989 *Phys. Scr.* **39** 562.

[52] Chou H S, Chi H C, and Huang K N 1994 *Phys. Rev.* A **49** 2394.
[53] Utter S B, Beiersdorfer P, and Träbert E 2003 *Can. J. Phys.* **81** 911.
[54] Träbert E, Beiersdorfer P and Chen H 2004 *Phys. Rev.* A **70** 032506.
[55] Vilkas M J and Ishikawa Y 2005 *Phys. Rev.* A **72** 032512.
[56] Blundell S A, Johnson W R, Safronova M S and Safronova V I 2008 *Phys. Rev.* A **77** 032507.
[57] Blundell S A 2009 *Can. J. Phys.* **87** 55.
[58] Fischer C F and Hansen J G 1978 *Phys. Rev.* A **17** 1956.
[59] Huang K N and Johnson W R 1985 *Nucl. Instrum. Methods* **B9** 502.
[60] Fleming J and Hibbert A 1995 *Phys. Scr.* **51** 339.
[61] Johnson W R and Soff G 1985 *At. Data Nucl. Data Tables* **33** 405.
[62] Zumbro J D, Naumann R A, Hoehn M V, Shera E B, Bemis Jr. C E, and Tanaka Y 1986 *Phys. Lett.* **167B** 383.
[63] Zumbro J D, Shera E B, Tanaka Y, Bemis Jr. C E, Naumann R A, Hoehn, Reuter W and Steffen R M 1984 *Phys. Rev. Lett.* **53** 1888.
[64] Seely J F, Brown C M, Feldman U 1989 *At. Data Nucl. Data Tables* **43** 145.
[65] Utter S B, Beiersdorfer P, Träbert E and Clothiaus E J 2003 *Phys. Rev.* A **67** 032502.
[66] Cheng K T and Chen M H 2006 *Rad. Phys. Chem.* **75** 1753.
[67] McElroy T and Hibbert A 2005 *Phys. Scr.* **71** 479.
[68] Hibbert A and Bailie A C 1992 *Phys. Scr.* **45** 565.
[69] Landman A and Novick R 1964 *Phys. Rev.* **134** A56.
[70] Baumann S R, and Smith W H 1970 *J. Opt. Soc. Am* **60** 345.
[71] Andersen T and Sorensen G 1973 *J. Quant. Spectrosc. Radiat. Transfer* **13** 369.
[72] Lurio A, deZafra R L and Goshen R J 1964 *Phys. Rev.* **134** A1198.
[73] Andersen T, Eriksen P, Poulsen O and Ramanujam P S 1979 *Phys. Rev.* A **20** 2621.
[74] Ansbacher W, Pinnington E H, Hahr J L and Kernahan J A 1985, *Can. J. Phys.* **63** 1330.
[75] Sorensen G 1973 *Phys. Rev.* A **7** 85.
[76] Pinnington E H, Bahr J L, Kernahan J A and Irwin D J G 1981 *J. Phys. B: At. Mol. Opt. Phys.* **14** 1291.
[77] Bahr J L, Pinnington E H, Kernahan J A, and O'Neill J A 1982, *Can. J. Phys.* **60** 1108.
[78] Pinnington E H, Kernahan J A and Donnelly K E 1977 *J. Opt. Soc. Am.* **67** 162.
[79] Knystautas E J and Drouin R 1977 *J. Quant. Spectrosc. Radiat. Transfer* **17** 551.
[80] Irwin D J G, Kernahan J A, Pinnington E H and Livingston A E 1976 *J. Opt. Soc. Am.* **66** 1396.
[81] Druetta M and Buchet J P 1976 *J. Opt. Soc. Am* **66** 433.
[82] Pinnington E H, Ansbacher W and Kernahan J A 1984 *J. Opt. Soc. Am.* **B1** 30.
[83] Heckmann P H, Moller G, Träbert E, Wagner C, Martinson I, Blanke J H and Sugar J 1991 *Phys. Scr.* **44** 151.
[84] Träbert E, Heckmann P H, Doerfert J and Granzow J 1993 *Phys. Scr.* **47** 780.
[85] Träbert E and Pinnington E H 1993 *Can. J. Phys.* **71** 128.
[86] Träbert E 1989 *Phys. Scr.* **39** 592.

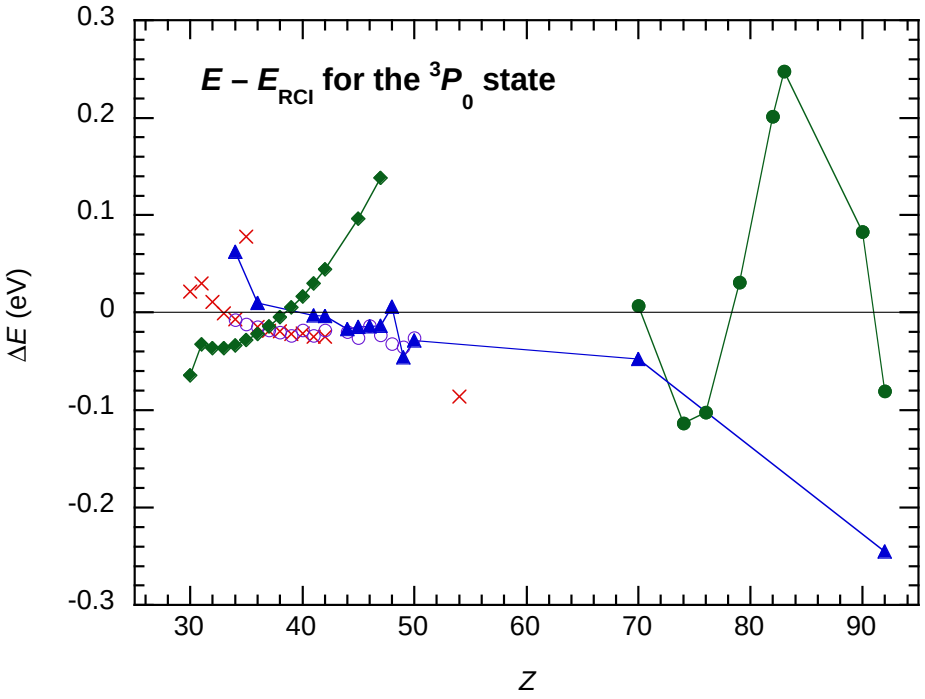

Figure 1. Experimental and theoretical excitation energies relative to the present RCI results for the $^3P_0$ state of Zn-like ions. Symbols for experiments are given by: crosses from NIST database [35] and Litzen and Reader [36]; open circles from Joshi and van Kleef [37], Trigueiros *et al* [38] and Churilov *et al* [39]. Symbols for theories are connected by lines and are given by: solid diamonds from Liu *et al* [40]; solid circles from Vilkas and Ishikawa [55]; solid triangles from Blundell *et al* [56].

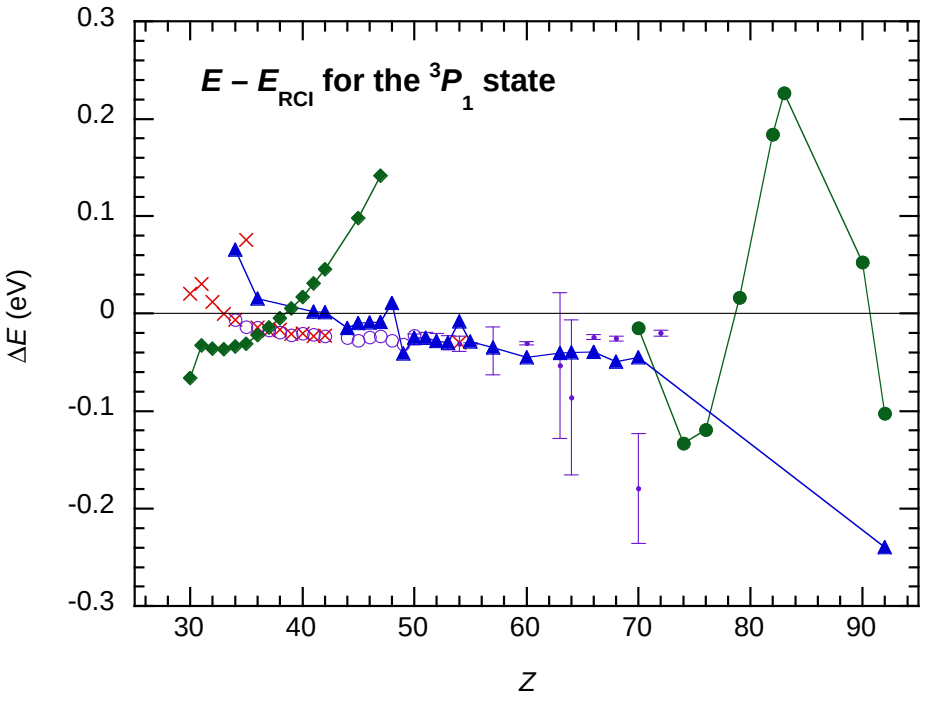

Figure 2. Experimental and theoretical excitation energies relative to the present RCI results for the $^3P_1$ state of Zn-like ions. Dots with error bars are from Brown *et al* [44]. Other symbols are the same as those in figure 1.

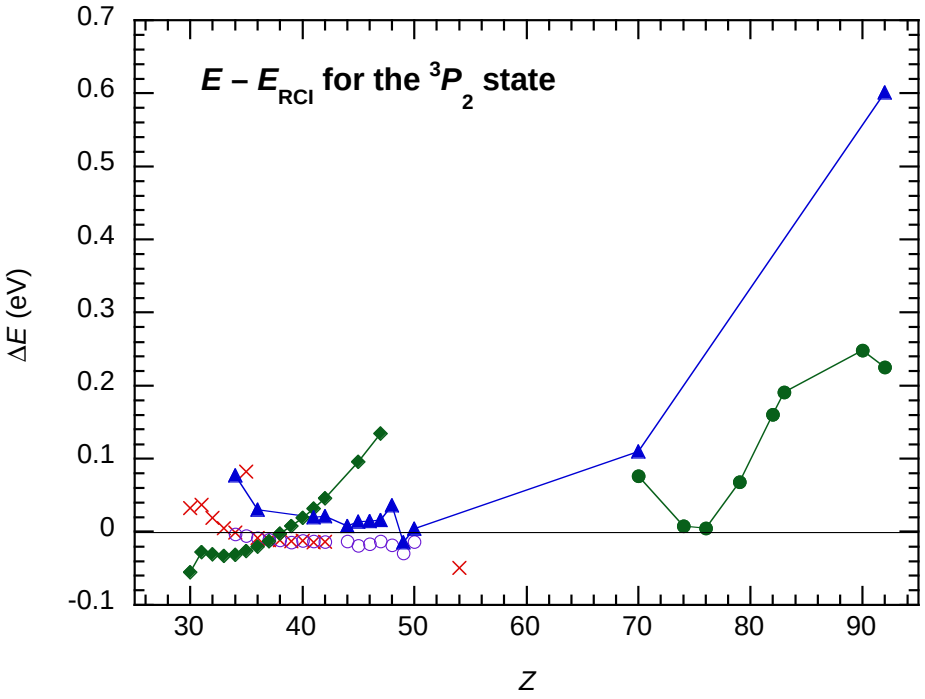

Figure 3. Experimental and theoretical excitation energies relative to the present RCI results for the $^3P_2$ state of Zn-like ions. Symbols are the same as those in figure 1.

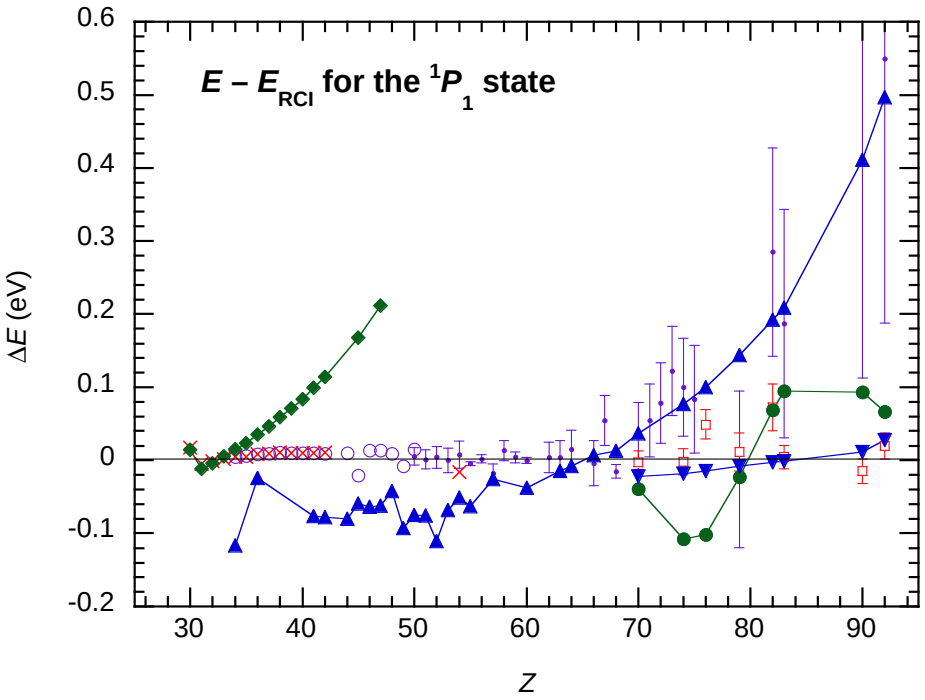

Figure 4. Experimental and theoretical excitation energies relative to the present RCI results for the $^1P_1$ state of Zn-like ions. Dots with error bars are from Brown *et al* [44]. Open squares with error bars are from Träbert *et al* [54] Solid down-triangles connected by lines are from Blundell [57]. Other symbols are the same as those in figure 1.

Table 1. Contributions to the excitation energies (eV) of the $4s4p$ states in Zn-like ions. Coul, B_0 and B_ω are Coulomb, frequency-independent and frequency-dependent Breit energies, respectively. SE, UP, WK, RX and HO are self-energy, Uehling potential, Wichmann-Kroll, relaxation and high-order contributions to the QED energies, respectively.

Terms	Kr^{6+}	Xe^{24+}	Yb^{40+}	U^{62+}	Kr^{6+}	Xe^{24+}	Yb^{40+}	U^{62+}
	$^3P_0$				$^3P_1$			
Coul	14.581	46.287	78.000	131.331	14.921	49.245	84.127	141.976
B_0	0.022	0.250	0.824	2.621	0.015	0.225	0.778	2.522
B_ω	0.000	-0.001	0.002	0.074	0.000	-0.003	0.000	0.072
Breit	0.021	0.249	0.826	2.694	0.015	0.222	0.778	2.594
RCI	14.602	46.536	78.826	134.025	14.936	49.467	84.905	144.570
SE	-0.037	-0.377	-1.245	-4.164	-0.036	-0.375	-1.245	-4.167
UP	0.003	0.048	0.205	1.005	0.003	0.048	0.205	1.006
WK	0.000	-0.001	-0.007	-0.045	0.000	-0.001	-0.007	-0.045
RX	0.000	0.000	-0.005	-0.024	0.001	0.000	-0.005	-0.024
HO	0.000	0.000	0.003	0.015	0.000	0.000	0.003	0.015
QED	-0.033	-0.330	-1.049	-3.212	-0.032	-0.328	-1.049	-3.215
Total	14.569	46.206	77.777	130.813	14.904	49.139	83.856	141.355
	$^3P_2$				$^1P_1$			
Coul	15.730	64.399	153.216	454.857	21.204	75.715	169.028	477.361
B_0	0.000	0.011	0.007	-0.396	0.002	0.020	0.021	-0.349
B_ω	-0.001	-0.023	-0.108	-0.518	-0.001	-0.021	-0.106	-0.514
Breit	-0.001	-0.012	-0.101	-0.914	0.001	-0.001	-0.085	-0.863
RCI	15.730	64.387	153.115	453.944	21.204	75.715	168.944	476.498
SE	-0.035	-0.350	-1.175	-4.253	-0.036	-0.355	-1.183	-4.264
UP	0.004	0.050	0.224	1.231	0.004	0.050	0.225	1.233
WK	0.000	-0.001	-0.007	-0.059	0.000	-0.001	-0.007	-0.059
RX	0.001	0.002	0.005	0.030	0.001	0.001	0.005	0.030
HO	0.000	0.000	0.003	0.015	0.000	0.000	0.003	0.015
QED	-0.031	-0.299	-0.951	-3.036	-0.032	-0.305	-0.958	-3.045
Total	15.699	64.088	152.164	450.908	21.172	75.410	167.986	473.453

Table 2. Excitation energies (eV) relative to the ground state for the $4s4p\ ^3P_0$ levels in Zn-like ions.

Z	RCI	QED	Total	Z	RCI	QED	Total
30	3.9893	-0.005	3.9846	62	62.056	-0.620	61.435
31	5.8503	-0.008	5.8426	63	64.077	-0.666	63.412
32	7.6540	-0.011	7.6427	64	66.118	-0.713	65.405
33	9.4161	-0.016	9.4005	65	68.181	-0.763	67.418
34	11.155	-0.021	11.135	66	70.266	-0.815	69.450
35	12.882	-0.027	12.856	67	72.367	-0.870	71.498
36	14.602	-0.033	14.569	68	74.501	-0.927	73.574
37	16.320	-0.040	16.280	69	76.651	-0.987	75.664
38	18.037	-0.048	17.989	70	78.826	-1.049	77.777
39	19.757	-0.058	19.700	71	81.028	-1.114	79.914
40	21.481	-0.067	21.413	72	83.253	-1.182	82.071
41	23.209	-0.078	23.131	73	85.507	-1.252	84.255
42	24.944	-0.090	24.854	74	87.783	-1.326	86.458
43	26.686	-0.103	26.583	75	90.094	-1.402	88.692
44	28.436	-0.117	28.319	76	92.429	-1.481	90.948
45	30.195	-0.133	30.062	77	94.794	-1.564	93.230
46	31.964	-0.149	31.815	78	97.189	-1.649	95.540
47	33.743	-0.167	33.576	79	99.615	-1.738	97.876
48	35.532	-0.186	35.347	80	102.07	-1.830	100.24
49	37.334	-0.206	37.128	81	104.56	-1.926	102.63
50	39.148	-0.228	38.920	82	107.08	-2.025	105.05
51	40.975	-0.251	40.724	83	109.63	-2.127	107.50
52	42.814	-0.276	42.538	84	112.22	-2.233	109.98
53	44.669	-0.302	44.366	85	114.83	-2.343	112.49
54	46.536	-0.330	46.206	86	117.47	-2.456	115.02
55	48.419	-0.360	48.059	87	120.16	-2.573	117.59
56	50.317	-0.392	49.925	88	122.88	-2.693	120.19
57	52.231	-0.425	51.806	89	125.64	-2.817	122.82
58	54.161	-0.460	53.701	90	128.37	-2.945	125.43
59	56.108	-0.497	55.611	91	131.26	-3.077	128.18
60	58.073	-0.536	57.536	92	134.03	-3.212	130.81
61	60.055	-0.577	59.478				

Table 3. Excitation energies (eV) relative to the ground state for the $4s4p\ ^3P_1$ levels in Zn-like ions.

Z	RCI	QED	Total	Z	RCI	QED	Total
30	4.0141	-0.005	4.0094	62	66.546	-0.619	65.927
31	5.9050	-0.008	5.8975	63	68.766	-0.664	68.102
32	7.7480	-0.011	7.7369	64	71.004	-0.712	70.292
33	9.5577	-0.015	9.5423	65	73.265	-0.762	72.503
34	11.353	-0.020	11.333	66	75.549	-0.814	74.734
35	13.146	-0.026	13.120	67	77.849	-0.869	76.980
36	14.936	-0.032	14.904	68	80.182	-0.926	79.255
37	16.736	-0.039	16.696	69	82.531	-0.986	81.544
38	18.543	-0.048	18.496	70	84.905	-1.049	83.856
39	20.362	-0.056	20.306	71	87.306	-1.114	86.193
40	22.194	-0.066	22.127	72	89.731	-1.182	88.550
41	24.038	-0.077	23.961	73	92.185	-1.252	90.933
42	25.898	-0.089	25.809	74	94.662	-1.326	93.336
43	27.773	-0.102	27.671	75	97.173	-1.402	95.771
44	29.663	-0.116	29.548	76	99.710	-1.482	98.228
45	31.569	-0.131	31.439	77	102.28	-1.565	100.71
46	33.492	-0.147	33.345	78	104.87	-1.650	103.22
47	35.430	-0.165	35.265	79	107.50	-1.739	105.76
48	37.385	-0.184	37.201	80	110.16	-1.832	108.32
49	39.356	-0.204	39.152	81	112.85	-1.927	110.92
50	41.345	-0.226	41.120	82	115.57	-2.026	113.55
51	43.351	-0.249	43.102	83	118.33	-2.129	116.20
52	45.373	-0.274	45.099	84	121.12	-2.235	118.89
53	47.412	-0.300	47.112	85	123.94	-2.344	121.60
54	49.467	-0.328	49.139	86	126.79	-2.457	124.33
55	51.539	-0.358	51.182	87	129.68	-2.574	127.11
56	53.629	-0.389	53.240	88	132.61	-2.695	129.91
57	55.737	-0.423	55.314	89	135.57	-2.819	132.75
58	57.862	-0.458	57.404	90	138.51	-2.947	135.56
59	60.006	-0.495	59.510	91	141.60	-3.079	138.52
60	62.167	-0.534	61.633	92	144.57	-3.215	141.36
61	64.347	-0.576	63.771				

Table 4. Excitation energies (eV) relative to the ground state for the $4s4p\ ^3P_2$ levels in Zn-like ions.

Z	RCI	QED	Total	Z	RCI	QED	Total
30	4.0500	-0.005	4.0453	62	100.65	-0.561	100.09
31	6.0147	-0.007	6.0073	63	106.19	-0.602	105.59
32	7.9448	-0.011	7.9342	64	111.99	-0.645	111.35
33	9.8651	-0.015	9.8505	65	118.07	-0.690	117.38
34	11.794	-0.019	11.775	66	124.44	-0.737	123.71
35	13.746	-0.025	13.721	67	131.11	-0.787	130.33
36	15.730	-0.031	15.699	68	138.11	-0.839	137.27
37	17.753	-0.037	17.716	69	145.44	-0.893	144.54
38	19.823	-0.045	19.778	70	153.11	-0.951	152.16
39	21.946	-0.053	21.893	71	161.16	-1.010	160.15
40	24.128	-0.062	24.066	72	169.59	-1.072	168.52
41	26.375	-0.072	26.303	73	178.43	-1.138	177.29
42	28.692	-0.083	28.609	74	187.68	-1.206	186.48
43	31.086	-0.094	30.992	75	197.39	-1.276	196.11
44	33.563	-0.107	33.456	76	207.55	-1.350	206.20
45	36.130	-0.121	36.009	77	218.20	-1.428	216.77
46	38.792	-0.136	38.656	78	229.36	-1.508	227.85
47	41.557	-0.152	41.405	79	241.05	-1.592	239.45
48	44.431	-0.169	44.262	80	253.28	-1.679	251.61
49	47.422	-0.187	47.235	81	266.11	-1.769	264.34
50	50.536	-0.207	50.329	82	279.54	-1.864	277.68
51	53.782	-0.228	53.554	83	293.60	-1.962	291.64
52	57.166	-0.250	56.916	84	308.34	-2.064	306.27
53	60.699	-0.274	60.425	85	323.76	-2.170	321.59
54	64.387	-0.299	64.088	86	339.89	-2.280	337.61
55	68.240	-0.326	67.914	87	356.81	-2.395	354.41
56	72.267	-0.354	71.913	88	374.51	-2.513	372.00
57	76.478	-0.384	76.094	89	393.05	-2.637	390.42
58	80.882	-0.416	80.467	90	412.39	-2.765	409.63
59	85.491	-0.449	85.042	91	432.78	-2.898	429.88
60	90.315	-0.485	89.831	92	453.94	-3.036	450.91
61	95.365	-0.522	94.844				

Table 5. Excitation energies (eV) relative to the ground state for the $4s4p\ 4s4p\ ^1P_1$ levels in Zn-like ions.

Z	RCI	QED	Total	Z	RCI	QED	Total
30	5.7836	-0.005	5.7786	62	114.19	-0.567	113.63
31	8.7789	-0.008	8.7711	63	120.01	-0.608	119.41
32	11.403	-0.011	11.392	64	126.10	-0.651	125.45
33	13.903	-0.015	13.887	65	132.46	-0.697	131.76
34	16.349	-0.020	16.328	66	139.11	-0.744	138.37
35	18.777	-0.026	18.751	67	146.07	-0.794	145.28
36	21.204	-0.032	21.172	68	153.36	-0.846	152.51
37	23.648	-0.039	23.610	69	160.97	-0.900	160.07
38	26.119	-0.047	26.073	70	168.94	-0.958	167.99
39	28.627	-0.055	28.572	71	177.29	-1.017	176.27
40	31.178	-0.064	31.114	72	186.01	-1.080	184.93
41	33.781	-0.074	33.706	73	195.15	-1.145	194.00
42	36.443	-0.086	36.358	74	204.70	-1.213	203.49
43	39.172	-0.098	39.074	75	214.71	-1.284	213.42
44	41.973	-0.111	41.863	76	225.17	-1.358	223.81
45	44.855	-0.125	44.730	77	236.12	-1.435	234.69
46	47.825	-0.140	47.685	78	247.58	-1.516	246.07
47	50.890	-0.156	50.735	79	259.57	-1.599	257.98
48	54.060	-0.173	53.886	80	272.12	-1.686	270.43
49	57.341	-0.192	57.149	81	285.25	-1.777	283.48
50	60.743	-0.212	60.531	82	298.99	-1.872	297.12
51	64.272	-0.233	64.039	83	313.37	-1.970	311.40
52	67.938	-0.255	67.682	84	328.41	-2.072	326.34
53	71.749	-0.279	71.470	85	344.14	-2.178	341.96
54	75.714	-0.305	75.410	86	360.59	-2.288	358.30
55	79.844	-0.332	79.513	87	377.82	-2.403	375.41
56	84.147	-0.360	83.787	88	395.83	-2.522	393.31
57	88.634	-0.390	88.244	89	414.68	-2.645	412.04
58	93.315	-0.422	92.893	90	434.33	-2.774	431.56
59	98.200	-0.456	97.744	91	455.03	-2.907	452.12
60	103.30	-0.491	102.81	92	476.50	-3.045	473.45
61	108.63	-0.528	108.10				

Table 6. QED corrections (eV) for the $^1P_1$ excitation energies of Zn-like ions.

Z	This work	Blundell *et al* [a]	Blundell[b]
51	-0.233	-0.256	
52	-0.255	-0.279	
53	-0.279	-0.303	
54	-0.305	-0.328	
55	-0.332	-0.355	
57	-0.390	-0.414	
60	-0.491	-0.516	
63	-0.608	-0.634	
64	-0.651	-0.678	
66	-0.744	-0.772	
68	-0.846	-0.875	
70	-0.958	-0.988	-0.939
74	-1.213	-1.249	-1.192
76	-1.358	-1.397	-1.334
79	-1.599	-1.643	-1.573
82	-1.872	-1.922	-1.839
83	-1.970	-2.023	-1.938
90	-2.774	-2.852	-2.729
92	-3.045	-3.132	-2.994

[a] Ref. [56].
[b] Ref. [57].

Table 7. Frequency-dependent, retarded Breit energies (eV) for the $^1P_1$ excitation energies of Zn-like ions. Diagonal and off-diagonal contributions are the present RCI results. RMBPT energies are from Blundell [57].

Z	Diagonal	Off-diagonal	RMBPT
70	-0.110	0.004	-0.109
74	-0.153	0.006	-0.152
76	-0.179	0.006	-0.178
79	-0.224	0.008	-0.223
82	-0.277	0.010	-0.276
83	-0.297	0.010	-0.296
90	-0.470	0.016	-0.470
92	-0.532	0.018	-0.532

Table 8. E1 transition rates (s^{-1}) for the $4s^2\ ^1S_0 - 4s4p\ ^{3,1}P_1$ transitions in Zn-like ions. Numbers in parentheses represent powers of 10.

Z	$^3P_1$	$^1P_1$	Z	$^3P_1$	$^1P_1$
30	4.47(4)	7.35(8)	62	7.33(9)	1.95(11)
31	2.65(5)	1.88(9)	63	8.00(9)	2.14(11)
32	9.89(5)	3.15(9)	64	8.71(9)	2.36(11)
33	2.67(6)	4.59(9)	65	9.43(9)	2.60(11)
34	5.97(6)	6.22(9)	66	1.02(10)	2.87(11)
35	1.18(7)	8.01(9)	67	1.10(10)	3.16(11)
36	2.11(7)	9.99(9)	68	1.18(10)	3.49(11)
37	3.53(7)	1.21(10)	69	1.26(10)	3.85(11)
38	5.60(7)	1.45(10)	70	1.35(10)	4.25(11)
39	8.51(7)	1.70(10)	71	1.43(10)	4.70(11)
40	1.24(8)	1.97(10)	72	1.52(10)	5.19(11)
41	1.76(8)	2.26(10)	73	1.62(10)	5.74(11)
42	2.43(8)	2.58(10)	74	1.71(10)	6.36(11)
43	3.28(8)	2.92(10)	75	1.81(10)	7.04(11)
44	4.32(8)	3.29(10)	76	1.91(10)	7.79(11)
45	5.59(8)	3.68(10)	77	2.01(10)	8.63(11)
46	7.10(8)	4.11(10)	78	2.12(10)	9.56(11)
47	8.88(8)	4.57(10)	79	2.22(10)	1.06(12)
48	1.09(9)	5.07(10)	80	2.33(10)	1.18(12)
49	1.33(9)	5.61(10)	81	2.45(10)	1.30(12)
50	1.60(9)	6.19(10)	82	2.56(10)	1.45(12)
51	1.90(9)	6.83(10)	83	2.68(10)	1.61(12)
52	2.23(9)	7.52(10)	84	2.80(10)	1.78(12)
53	2.59(9)	8.28(10)	85	2.92(10)	1.98(12)
54	2.99(9)	9.11(10)	86	3.04(10)	2.20(12)
55	3.42(9)	1.00(11)	87	3.17(10)	2.44(12)
56	3.89(9)	1.10(11)	88	3.30(10)	2.71(12)
57	4.38(9)	1.21(11)	89	3.43(10)	3.01(12)
58	4.91(9)	1.33(11)	90	3.56(10)	3.35(12)
59	5.47(9)	1.46(11)	91	3.71(10)	3.73(12)
60	6.06(9)	1.61(11)	92	3.84(10)	4.14(12)
61	6.68(9)	1.77(11)			

Table 9. Lifetime (ns) for the $4s^2\ ^1S_0 - 4s4p\ ^1P_1$ transition in Zn-like ions. Numbers in parentheses indicate uncertainties of experiment.

Z	RCI[a]	MCDF[b]	CIV3	MCRRPA[c]	MCHF[d]	Expt	Ref
30	1.361	1.316			1.320	1.38(0.05)	[69]
						1.75(0.20)	[70]
						1.45(0.15)	[71]
						1.41(0.04)	[72]
31	0.532	0.531	0.528[e]	0.483	0.514	0.49(0.04)	[73]
						0.48(0.12)	[74]
						0.65(0.08)	[75]
32	0.318	0.315		0.293	0.306	0.29(0.03)	[73]
						0.39(0.06)	[75]
33	0.218	0.216		0.203	0.210	0.23(0.03)	[73]
						0.32(0.08)	[75]
						0.26(0.05)	[76]
34	0.161	0.159			0.154	0.27(0.05)	[75]
						0.20(0.02)	[77]
35	0.125	0.124		0.118	0.120	0.24(0.04)	[78]
						0.24(0.02)	[79]
36	0.100	0.0991	0.103[f]	0.0953	0.0958	0.19(0.02)	[79]
						0.163(0.06)	[80]
						0.19(0.02)	[81]
						0.101(0.010)	[82]
37	0.0824	0.0816		0.0787			
38	0.0691	0.0685					
39	0.0589	0.0583					
40	0.0507	0.0503					
41	0.0442	0.0438		0.0425			
42	0.0388	0.0384		0.0374	0.0371		
45	0.0272	0.0270					
47	0.0219	0.0217		0.0212			
48	0.0197			0.0191	0.0158		
50	0.0161				0.0158		
53	0.0121			0.0117			
54	0.0110			0.0107			
55	0.0100			0.00972			
56	0.00908			0.00885			
62	0.00513				0.00473		
74	0.00157				0.00143		

[a] This work.
[b] Liu *et al* [40].
[c] Chou *et al* [52].
[d] Fischer and Hansen [58].
[e] McElroy and Hibbert [67].
[f] Hibbert and Bailie [68].

Table 10. Lifetime (ns) for the $4s^2\ ^1S_0 - 4s4p\ ^3P_1$ transition in Zn-like ions. Here, me and cm are multi-exponent and cascade mode fits, respectively, in determining experimental data. Numbers in parentheses indicate uncertainties of experiment.

Z	RCI[a]	MCDF[b]	CIV3[c]	MCRRPA[d]	Expt	Fit	Ref
30	22375	25490		32971			
31	3774	3545	3090[e]	4138			
			2445				
32	1011	975.6		1089			
33	374.1	366.6		399.2			
34	167.5	165.6					
35	85.10	84.61		88.01			
36	47.45	47.30	46.19	49.81	47(10)	me	[82]
37	28.31	28.29		29.61			
38	17.85	17.85	16.82				
39	11.76	11.70					
40	8.03	8.05					
41	5.67	5.68	5.49	6.08	6.45(0.40)	me	[83]
					5.6(0.4)	me	[84]
42	4.11	4.12	3.99	4.22	3.73(0.20)	me	[85]
					3.6(0.2)	cm	[85]
					4.5(0.3)	me	[86]
45	1.79	1.79	1.75		1.9(0.2)	me	[84]
					1.55(0.20)	cm	[84]
47	1.13	1.13	1.12	1.14	1.18(0.08)	me	[86]
					1.2(0.1)	me	[84]
					1.04(0.06)	cm	[84]
48	0.914			0.926			
54	0.334			0.335			

[a] This work.
[b] Liu *et al* [40].
[c] Fleming and Hibbert [60] unless otherwise specified.
[d] Chou *et al* [52].
[e] McElroy and Hibbert [67].